Cell-free Massive MIMO Systems under Jamming Attack

Ramiz Sabbagh*, Huiling Zhu, and Jiangzhou Wang
School of Engineering and Digital Arts, University of Kent, Canterbury, CT2 7NT, United Kingdom
Email: ramizsabbagh@gmail.com, {h.zhu and j.z.wang}@kent.ac.uk

***Abstract*—This paper evaluates the uplink spectral efficiency (SE) performance of a cell-free massive multiple-input-multiple-output (MIMO) network under the attack of several distributed jammers. The signal-to-interference-plus-noise ratio (SINR) formula for the maximum-ratio-combining (MRC) receiver is initially derived for an arbitrary legitimate user-equipment (UE) by considering the harmful impact of jammers. These jammers target the access points (APs) during both training and data transmissions. Two power control methods are developed to improve the SE performance, a max-min one aiming to ensure uniformly good service for UEs, and a second method aiming to achieve proportional fairness. The proposed system is compared with a single cell co-located massive MIMO system, and with another cell-free massive MIMO system including smart jammers, provided with the legitimate UEs' pilot signals. Simulation results demonstrate the superiority of the proportional fairness power control compared with the max-min fairness and the other scenarios under the threat of jammers. The effect of the number of jammers and their transmission power is further presented and analysed.**

1. Introduction

Cell-free massive multiple-input multiple-output (MIMO) is introduced as a promising technique to meet the high demands of the future wireless networks in terms of spectral efficiency and coverage [1]. The structure of the cell-free network includes distributing a large number of access points (APs) over a wide area to jointly serve multiple user-equipments (UEs) in the same time/frequency resource without using the limitations of cells. A central processing unit (CPU) is additionally employed to manage the cooperation among the APs [1], [2].

The ability to completely exploit the space micro-diversity and macro-diversity can enable the cell-free massive MIMO to achieve a very high probability of coverage compared to that of co-located massive MIMO [3], [4]. Similarly to the latter, cell-free can still provide favourable propagation and channel hardening properties, resulting in the mitigation of the inter-user interference and offering higher spectral efficiency [5]. The simplicity of signal precessing is another merit of cell-free systems, as local channel state information (CSI) is required at the APs and low-complexity conjugated precoding is applied. Therefore, only a limited information exchange between CPU and the APs is needed. This results in a system with an ability to scale up, and with a relatively low overhead [6].

In recent years, several aspects related to cell-free massive MIMO have been actively studied, including performance analysis, beamforming, power control and pilot designs [5]–[8]. However, physical layer security in cell-free massive MIMO has not been well investigated, especially in the case of multiple jamming attacks. Although cell-free massive MIMO has several advantages as mentioned above, it suffers during a jamming attack when the attack occurs in the training phase. As a result, the spectral efficiency (SE) of the massive MIMO systems can be significantly degraded [9].

In the literature, there are some researches on the security issue in the cell-free massive MIMO [10]–[12]. Two of these works [10], [11] dealt with the presence of an active eavesdropper, which can be seen as a jammer transmitting disturbing signals during the pilot phase to interfere the process of channel estimation and to improve the precision of the wiretap. In [12], the downlink spectral efficiency in the existence of an active eavesdropper was derived and compared with that of a passive eavesdropper, and an algorithm for transmit power allocation for APs was developed to reduce the rate leaked into the eavesdropper. However, all the aforementioned works [10]–[12] included only a single eavesdropper. The authors of [13] considered a single cell co-located massive MIMO network with several jammers, where techniques for jammer detecting and mitigating were developed based on random matrix theory. A similar setup with distributed jammers was adopted in [14], where the uplink SE was analysed and compared with that of a single-user single-input multiple-output (SIMO) system within different power control schemes. Unfortunately, the analysis and the methods proposed in both [13] and [14] cannot be extended to work in the cell-free massive MIMO.

In this paper, the uplink SE formula is derived for an individual UE in both a cell-free massive MIMO and a single cell co-located massive MIMO under the attack of multiple distributed jammers. This application is motivated by the fact that distributed jammers are more difficult to find and suppress than for a single jammer. Moreover, different comparisons are provided for the SE performance of cell-free massive MIMO, with and without smart jammers, to that of co-located massive MIMO systems. These comparisons are made under an increasing number of jammers while keeping their total power fixed. It is further considered that the jammers are attacking the APs in both training and data phases. The contribution of this paper is summarised as follows:

1) A closed-form uplink signal-to-interference-plus-noise ratio (SINR) formula is derived for the cell-free massive

*Ramiz Sabbagh is also with the Communication Engineering Department, Ninevah University, Mosul, 41002, Iraq.

MIMO. Furthermore, the SINR expressions are provided for a single cell massive MIMO system and for cell-free massive MIMO with smart jammers which know the pilot signals. The minimum mean square error (MMSE) estimator and the maximum-ratio-combining (MRC) receiver are employed in these derivations.

2) Based on the derived SINR, under the UEs' quality of service (QoS) constraints, two power control methods are developed to maximise the minimum SINR and to provide proportional fairness, respectively.
3) The uplink SE performance of an arbitrary UE in the cell-free massive MIMO is compared with these of the co-located massive MIMO and the case of smart jammers, when a various number of jammers is considered.

Notations: boldface lower and upper case symbols refer to vectors and matrices, respectively. $(\cdot)^T$, $(\cdot)^*$ and $(\cdot)^H$ indicate transpose, conjugate and Hermitian transpose operators, respectively. $\mathbf{I}_N$ is a $N \times N$ identity matrix, and $\mathcal{CN}(\cdot,\cdot)$ is a circular-symmetric complex Gaussian distributed random variable. Finally, the notation $\mathbb{E}\{\cdot\}$ is the expectation.

2. System Model

A cell-free massive MIMO system is considered including M APs geographically distributed within the coverage area to serve K legitimate UEs using the same time-frequency resource. Both APs and UEs are equipped with a single antenna. It is assumed that each UE is served by all the APs in the network. The APs are linked to a CPU via perfect fronthaul links. It is further considered that J jammer devices are placed in the network aiming to send artificial noise signals. Each one of these jammers has a single antenna as well.

It is assumed that h_{mk} is the channel coefficient from the k^{th} UE to the m^{th} AP. Similarly, g_{mj} is the channel coefficient from the j^{th} jammer to the m^{th} AP. These channel coefficients are independent and identically distributed circular-symmetric complex Gaussian random variables, which means a model of Rayleigh fading channel is invoked in this paper [15], [16]. The channel responses h_{mk} and g_{mj} follow $\mathcal{CN}(0,\beta_{mk})$ and $\mathcal{CN}(0,\bar{\beta}_{mj})$, respectively, where β_{mk} and $\bar{\beta}_{mj}$ model the large-scale components of the k^{th} UE and the j^{th} jammer, respectively. In the two cases, the large-scale components include both the path-loss and the shadowing. The channel realisations h_{mk} and g_{mj} are independent, and also change independently from one coherence interval to another.

A. Channel State Information Acquisition

Uplink and downlink transmissions are conducted via the time division duplex (TDD) protocol. The coherence interval under TDD protocol has a phase for uplink training in addition to another two phases for uplink and download data transmissions. During the uplink training phase, the channel estimation is implemented in the APs by utilising the pilot signals sent synchronously by the legitimate UEs. For a coherence interval consisting of S symbols, B symbols are assigned for the pilot phase. The remaining $S-B$ symbols are kept for data transmission. It is additionally assumed that $B \geq K$, which enables each UE to obtain its unique orthogonal pilot signal. The pilot sequence of the k^{th} UE is defined as $\mathbf{q}_k \in \mathbb{C}^{B\times 1}$. The sequence of each UE is designed to be mutually orthogonal with the sequences of other UEs, such that, $\mathbf{q}_k^H\mathbf{q}_k = 1$ and $\mathbf{q}_k^H\mathbf{q}_{k'} = 0$, where $k \neq k'$, k and $k' \in \{1,\cdots,K\}$. The pilot vector obtained at the m^{th} AP, $\mathbf{y}_{p,m} \in \mathbb{C}^{B\times 1}$, is expressed as

$$\mathbf{y}_{p,m}=\sum_{k=1}^{K}\sqrt{B\rho_{p,k}}\,h_{mk}\mathbf{q}_k^T+\sum_{j=1}^{J}\sqrt{B\bar{\rho}_j}\,g_{mj}\mathbf{z}_j^T+\mathbf{n}_{p,m}, \quad (1)$$

where $\rho_{p,k}$ is the transmission pilot power of the k^{th} UE. $\bar{\rho}_j$ is also the transmission power of j^{th} jammer. $\mathbf{n}_{p,m} \sim \mathcal{CN}(0,\sigma_p^2)$ is the additive white Gaussian noise (AWGN) vector, received during the training phase. Finally, $\mathbf{z}_j$ denotes the attack signal belonging to the j^{th} jammer, transmitted during the pilot phase. The jammers prefer to generate $\mathbf{z}_j$ randomly so that $\mathbf{z}_j \sim \mathcal{CN}(\mathbf{0},\frac{1}{B}\mathbf{I}_B)$. This is necessary for the jammers to prevent the APs from estimating $\mathbf{z}_j$, which is the case if $\mathbf{z}_j$ is a deterministic vector. It is further assumed that these attack signals have independent realisation in every coherence interval.

To estimate the channel, h_{mt}, belonging to a particular UE t, $\mathbf{y}_{p,m}$ is initially projected along $\mathbf{q}_t$ to obtain the following,

$$\begin{aligned}\mathbf{c}_{mt} &= \mathbf{y}_{p,m}\mathbf{q}_t^*,\\ &= \sqrt{B\rho_{p,t}}\,h_{mt}+\sum_{j=1}^{J}\sqrt{B\bar{\rho}_j}\,g_{mj}\mathbf{z}_j^T\mathbf{q}_t^*+\mathbf{n}_{p,m}\mathbf{q}_t^*. \quad (2)\end{aligned}$$

The jammer-included MMSE estimate of h_{mt} is given by [17]

$$\hat{h}_{mt}^{\text{JI-MMSE}} = \frac{\sqrt{B\rho_{p,t}}\beta_{mt}}{B\rho_{p,t}\beta_{mt}+\sum_{j=1}^{J}\bar{\rho}_j\bar{\beta}_{mj}+\sigma_p^2}\mathbf{c}_{mt}. \quad (3)$$

If the CPU does not know the existence of the jammers' attack, the m^{th} AP estimates h_{mt} in the following way

$$\hat{h}_{mt} = \frac{\sqrt{B\rho_{p,t}}\beta_{mt}}{B\rho_{p,t}\beta_{mt}+\sigma_p^2}\mathbf{c}_{mt}, \quad (4)$$

which will be used in the rest of this paper. It should be noted that h_{mt} can be decomposed as $h_{mt} = \hat{h}_{mt}+\varepsilon_{mt}$, where ε_{mt} is the estimation error, which is uncorrelated with $\hat{h}_{mt}$ depending on the property of the MMSE estimation. Furthermore, both $\hat{h}_{mt}$ and ε_{mt} can be represented as $\mathcal{CN}(0,\theta_{mt})$ and $\mathcal{CN}(0,\beta_{mt}-\theta_{mt})$, respectively, where θ_{mt} is defined as [17]

$$\theta_{mt} = \frac{B\rho_{p,t}\beta_{mt}^2}{B\rho_{p,t}\beta_{mt}+\sigma_p^2}. \quad (5)$$

B. Uplink Data Transmission

Following the training phase, all K legitimate UEs send their data to the APs. However, the jammers aim to interfere legitimate UEs' data signals through sending disturbing signals. The received signal at the m^{th} AP is modelled as

$$y_{u,m} = \sum_{k=1}^{K}\sqrt{\rho_{u,k}}\,h_{mk}x_k+\sum_{j=1}^{J}\sqrt{\bar{\rho}_j}\,g_{mj}s_j+n_{u,m}, \quad (6)$$

where u indicates uplink data transmission. x_k is the transmitted symbol by the k^{th} UE, and s_j is the Gaussian signal transmitted by the j^{th} jammer which creates worst-case interference. Both x_k and s_j are assumed to have zero mean and unit

variance. $\rho_{u,k}$ is the uplink transmission power by the k^{th} UE. $n_{u,m}$ is the uplink AWGN, and is assumed to be $\mathcal{CN}(0, \sigma_u^2)$.

In order to decode the signal of the t^{th} UE, x_t, the m^{th} AP multiplies the received signal $y_{u,m}$ by the decoding coefficient, a_{mt}. The quantity obtained from the decoding processing for the t^{th} UE at the m^{th} AP is forwarded to the CPU through the fronthaul network. A similar decoding process is fulfilled by all other APs. Finally, the CPU receives the following signal

$$r_{u,t} = \sum_{m=1}^{M} a_{mt}^* y_{u,m} = \sum_{m=1}^{M} a_{mt}^* (\sqrt{\rho_{u,t}} h_{mt} x_t + \sum_{\substack{k=1, \\ k \neq t}}^{K} \sqrt{\rho_{u,k}} h_{mk} x_k + \sum_{j=1}^{J} \sqrt{\bar{\rho}_j} g_{mj} s_j + n_{u,m}). \quad (7)$$

By including the worst-case Gaussian method [18], the processed signal in (7), $r_{u,t}$, can be decomposed as

$$r_{u,t} = \mathrm{DS}_t x_t + \mathrm{IS}_1 x_t + \sum_{\substack{k=1, \\ k \neq t}}^{K} \mathrm{IS}_2 x_k + \sum_{j=1}^{J} \mathrm{JS}_t s_j + \mathrm{NS}_t, \quad (8)$$

where

$$\mathrm{DS}_t = \sqrt{\rho_{u,t}}\, \mathbb{E}\left[\sum_{m=1}^{M} a_{mt}^* h_{mt} \right], \quad (9a)$$

$$\mathrm{IS}_1 = \sqrt{\rho_{u,t}} \left(\sum_{m=1}^{M} a_{mt}^* h_{mt} - \mathbb{E}\left[\sum_{m=1}^{M} a_{mt}^* h_{mt} \right] \right), \quad (9b)$$

$$\mathrm{IS}_2 = \sqrt{\rho_{u,k}} \sum_{m=1}^{M} a_{mt}^* h_{mk}, \quad (9c)$$

$$\mathrm{JS}_t = \sqrt{\bar{\rho}_j} \sum_{m=1}^{M} a_{mt}^* g_{mj}, \quad (9d)$$

$$\mathrm{NS}_t = \sum_{m=1}^{M} a_{mt}^* n_{u,m}. \quad (9e)$$

Among the terms of (8), (9a) denotes the desired signal, while (9b) and (9c) are the effective interference. The signals from the J jammers are represented by (9d). (9e) is the effective noise which is uncorrelated with the desired signal. By considering the worst-case uncorrelated noise having a variance similar to that of the effective noise [18], the effective SINR for the t^{th} UE can be given by

$$\mathrm{SINR}_t = \frac{|\mathrm{DS}_t|^2}{\mathbb{E}[|\mathrm{IS}_1|^2] + \sum_{\substack{k=1, \\ k \neq t}}^{K} \mathbb{E}[|\mathrm{IS}_2|^2] + \sum_{j=1}^{J} \mathbb{E}[|\mathrm{JS}_t|^2] + \mathbb{E}[|\mathrm{NS}_t|^2]}. \quad (10)$$

The sum uplink SE can be represented by

$$\mathrm{R}_T = (1 - \frac{B}{S}) \sum_{k=1}^{K} \log_2(1 + \mathrm{SINR}_k). \quad (11)$$

C. MRC Receiver

In this subsection, the MRC detection is used, in which, a_{mt} is considered as $\hat{h}_{mt}$. After calculating the variances and expectations in (10), the SINR formula can be rewritten as in (12), at the top of the next page. The derivation of (12) can be found in Appendix A. In the case of setting the jammers' power coefficients $\rho_j,\ \forall j \in \{1, \cdots, J\}$ to zero, the SINR formula in (12) will coincide[1] with the uplink SINR expression of cell-free massive MIMO obtained in (Equation (27), [2]).

3. Additional Scenarios

In this section, two new scenarios are introduced for comparison purposes. That includes the co-located massive MIMO and the cell-free massive MIMO with smart jammers.

A. Co-located single cell massive MIMO

All APs in this scenario are assumed to be co-located. The SINR formula of the single cell co-located massive MIMO is deduced from the cell-free massive MIMO. Due to the distributed structure of the transmitting antennas in the cell-free massive MIMO, $\beta_{mk} \neq \beta_{m'k}$ and $\theta_{mk} \neq \theta_{m'k}$, for $m \neq m'$. However, this is not the case in the co-located massive MIMO, in which, $\beta_{mk} = \beta_{m'k} \triangleq \beta_k$ and $\theta_{mk} = \theta_{m'k} \triangleq \theta_k$, for $m \neq m'$. Consequently, the SINR expression for the co-located massive MIMO of the t^{th} UE can be written as in (13). Once again, if the jammers' power are set to zero, (13) precisely matches the uplink lower bound SINR expression for a single cell co-located massive MIMO obtained in (Chapter 3, [18]).

$$\mathrm{SINR}_t^{CO} = \frac{\rho_{u,t} M \theta_t}{\sum_{k=1}^{K} \rho_{u,k} \beta_k + \sum_{j=1}^{J} \bar{\rho}_j \bar{\beta}_j + \sigma_t^2} \quad (13)$$

B. Cell-free massive MIMO with smart jammers

In the system model previously presented in Section II, all jammers affected all pilot signals uniformally as shown in (1). In this subsection, a new scenario is considered, in which there are B smart jammers, and these jammers are provided with the pilot signals. All jammers are located in the same place in the network. Furthermore, every jammer is designed to target one of the legitimate UEs' pilot signals through sending a corresponding pilot sequence during the training phase. As a result, the formula in (2) can be rewritten as

$$\mathbf{c}_{mt} = \sqrt{B\rho_{p,t}}\ h_{mt} + \sqrt{B\bar{\rho}_j}\ g_{mj} + \mathbf{n}_{p,m} \mathbf{q}_t^*. \quad (14)$$

By considering the MRC detection, the SINR for the t^{th} UE can be obtained from (Equation (27), [2]). The reason is that the j^{th} smart jammer transmitting the same pilot of the t^{th} UE has an equivalent impact to the one of the pilot contamination in cell-free massive MIMO resulting from a UE sharing the pilot with UE t. Consequently, the effective SINR expression for the t^{th} UE can be expressed as shown in (15).

4. Power Control Design

An optimal design for both pilot and data power coefficients is presented in this section to improve the SE performance. The power control design is performed for the legitimate UEs in the cell-free massive MIMO network by utilising the MRC detection and under the impact of the jammers. As the CPU achieves power control, the CPU needs to know the powers of

[1]The impact of pilot contamination should be ignored while comparing (12) with (equation (27), [2]), as the pilot reuse is not considered in this paper.

$$\text{SINR}_t = \frac{\rho_{u,t}(\sum_{m=1}^{M}\theta_{mt})^2}{\sum_{k=1}^{K}\rho_{u,k}\sum_{m=1}^{M}\theta_{mt}\beta_{mk} + \sum_{j=1}^{J}\bar{\rho}_j\sum_{m=1}^{M}\theta_{mt}\bar{\beta}_{mj} + \sum_{m=1}^{M}\theta_{mt}\sigma_t^2} \tag{12}$$

$$\text{SINR}_t^{SJ} = \frac{\rho_{u,t}(\sum_{m=1}^{M}\theta_{mt})^2}{\bar{\rho}_j(\sum_{m=1}^{M}\theta_{mt}(\bar{\beta}_{mj}/\beta_{mt}))^2 + \sum_{k=1}^{K}\rho_{u,k}\sum_{m=1}^{M}\theta_{mt}\beta_{mk} + \sum_{m=1}^{M}\theta_{mt}\sigma_t^2} \tag{15}$$

the jammers' received signals. These powers can be estimated while the legitimate UEs remain silent [19]. Two optimisation problems are considered for the power control. The first one is the max-min, that aims to maximise the minimum SINR for all UEs, thereby providing all UEs with uniform good service, irrespective of their geographical locations. A second problem is further developed, which is proportional fairness, aiming to maximise the product of UEs' SINRs. Both these two problem require the closed-form SINR formula, which has been previously provided for the cell-free massive MIMO. The first problem of power control is given by

$$\begin{aligned} \mathcal{P}_1: \max_{\rho_{p,k},\rho_{u,k},\forall k} \quad & \zeta, \\ s.t. \ & \frac{\zeta}{\text{SINR}_k} \leq 1 \quad \forall k, \\ & \frac{B\rho_{p,k} + (S-B)\rho_{u,k}}{E_T} \leq 1 \quad \forall k. \end{aligned} \tag{16}$$

In (16), ζ is an auxiliary coefficient, and is designed so that, $\text{SINR}_k \geq \zeta, \ \forall k$. Specifically, ζ represents the SINR threshold which should be met by all UEs. E_T is the value of the total energy consumed within a single coherence interval.

The second problem is proportional fairness. This is equivalent to maximising the sum SE when the SINRs are much larger than 1. The formulation of this problem can be expressed as

$$\begin{aligned} \mathcal{P}_2: \max_{\rho_{p,k},\rho_{u,k},\forall k} \quad & \prod_{k=1}^{K}\mu_k, \\ s.t. \ & \frac{\mu_k}{\text{SINR}_k} \leq 1 \quad \forall k, \\ & \frac{B\rho_{p,k} + (S-B)\rho_{u,k}}{E_T} \leq 1 \quad \forall k. \end{aligned} \tag{17}$$

μ_k is an auxiliary coefficient for the k^{th} UE.

Both problems $\mathcal{P}_1$ and $\mathcal{P}_2$ are geometric programs (GP) [20]. The CVX package, which is a Matlab-based modelling system for convex optimisation, is used to solve these problems [21].

5. Simulation Results

In this section, the SE performance of cell-free Massive MIMO with the proposed power control designs is evaluated through simulation results and compared with different scenarios. The cell-free network is deployed in a 250×250 m^2 squared area. The APs, UEs and jammers are randomly and uniformly located in the defined area. It is assumed that $M = 64$ and $K = 12$. Each one of APs, UEs and jammers are equipped with a single-antenna. The UEs are served by all APs in this network. The third generation partnership project (3GPP) standard is utilised to model the large-scale fading, β_{mk} [22]. According to this standard, the path-loss is $148.1 + 37.6\log_{10} d_{mk}$ (dB), where d_{mk} denotes the distance from the m^{th} AP to the k^{th} UE calculated in km. The large-scale fading β_{mk} is then modelled as $\beta_{mk} = -148.1 - 37.6\log_{10} d_{mk} + z_{mk}$ (dB), where z_{mk} symbolises the shadow fading which has a lognormal distribution, and can be given by $10\log_{10}(z_{mk}) \sim \mathcal{CN}(0, \sigma_{shad}^2)$. The same large-scale model is used for $\bar{\beta}_{mj}$.

Unless otherwise mentioned, the other parameters are set as, $\sigma_{shad}^2 = 8$ dB, noise variance for both σ_p^2 and σ_k^2 is -96 dBm. The coherence block, $S = 200$, and the pilot block lengths, $B = 12$. The total energy per one coherence block is $E_T = 40$W, which means that the transmission power for pilots and data, $\rho_{p,k} = \rho_{u,k} = 200$ mW $\forall k$, in the case of full power transmission. The total transmission power for all jammers is 3.5W, and this power is distributed uniformally among the J available jammers. For instance, if $J = 5$, then $\bar{\rho}_j = 0.7$W $\forall j$, and if $J = 3$, then $\bar{\rho}_j$ is 1.17W $\forall j$. This applies to the case of smart jammers too, in which $J = 12$. In addition, all the aforementioned parameters apply to the scenario of co-located massive MIMO. For all simulation results, the simulation has iterated for 1000 times, where the locations of the APs, jammers and UEs changed in each iteration.

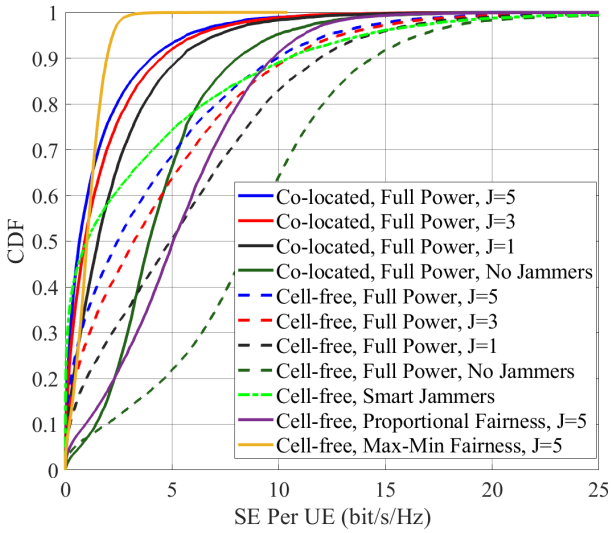

Fig. 1: CDF of uplink SE per UE for a cell-free massive MIMO ($K = 12$ and $M = 64$), and for a single cell co-located massive MIMO ($K = 12$ and $M = 64$).

Fig. 1 presents the cumulative distribution function (CDF) of the uplink SE per UE in the cell-free massive MIMO under the effect of various numbers of distributed jammers. Further two scenarios are included, the co-located massive MIMO and the cell-free with smart jammers. The simulation results clearly show that the SE performance of the cell-free is better than that of the co-located massive MIMO. For instance, a UE in cell-free system with 5 jammers can achieve a SE over 5 bit/s/Hz with probability 0.3. However, a UE in co-located massive MIMO can only reach a similar SE with much less probability

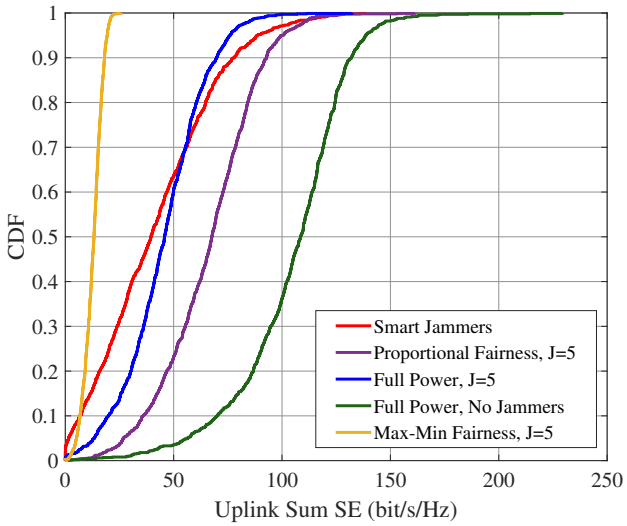

Fig. 2: CDF of uplink sum SE of a cell-free massive MIMO ($K = 12, M = 64$ and $J = 5$), and with $J = 12$ for the smart jammers case.

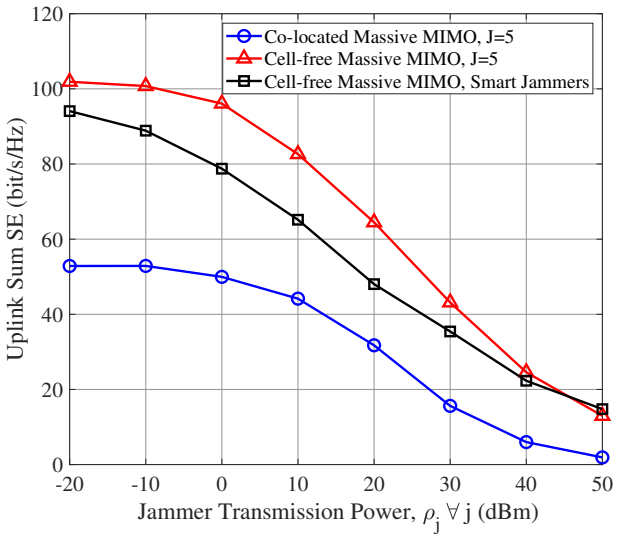

Fig. 3: The uplink sum SE versus jammer transmission power.

(around 0.05). For the full power case, although a fixed total power is utilised for all jammers regardless of how many they are, applying more jammers sharing this power will degrade the SE of UEs. This is due to that having more jammers increases the probability that each AP can have a nearby jammer, and this increases the jamming interfering power. In addition, the impact of the number of jammers is more significant in the cell-free system than that in the co-located system.

The performance of cell-free with smart jammers is mostly worse than that with 5 passive jammers with probability 0.9. As for each UE in the case of smart jammers, there is one jammer contaminating its channel estimate, causing a similar impact to that of pilot contamination resulting from pilot reuse. Finally, it can be seen that the proportional fairness improve the SE performance compared with the full power. The max-min fairness, however, provides poor SE compared with both the proportional fairness and the full power cases. Because in each realisation, one UE could have very low SINR due to jammers, which leads to low SINR for all other UEs.

The CDF of the uplink sum SE is further plotted in Fig. 2 for the cell-free massive scenario only. The performance of the proportional fairness is significantly better than the one of max-min fairness, as the aim in the proportional fairness is to improve the product of UEs SINR values, which is almost equivalent to maximising the sum SE. The max-min fairness presents another weak performance as if a UE is highly affected by the jamming attack causing low SINR, this will have negative impacts on the SINR of other UEs where they need to achieve the same poor SINR of the first unfortunate UE. Additionally, the performance of proportional fairness outperforms that of the full power with the same number of jammers. However, the full power case with 5 jammers is only able to outperform the smart jammers with probability 0.3.

Finally, Fig. 3 shows the impact of changing the jammer transmission power ($\bar{\rho}_j$) on the uplink sum SE for both cell-free and co-located massive MIMO networks. The power for all jammers is changed from -20 to 50 dBm in this figure. It can be noticed that before 0 dBm, changing the power has a minor impact on the sum SE for the co-located and cell-free massive MIMO with 5 passive jammers. Following that, the jammers start to considerably affect the sum SE. Under the smart jammers attack, the sum SE of the cell-free network continues to deduce while the power increases from -20 dBm. As a final finding, at $\bar{\rho}_j = 45$ dBm, the sum SE with 5 passive jammers will be equivalent to its counterpart of the smart jammers. This is due to the more severe impact that the smart jammers have on the SINR performance compared with that of the passive jammers, as shown in equations (12) and (15). Consequently, a number of passive jammers with sufficient power is needed to have the same impact on a UE SE to that of one smart jammer.

6. Conclusion

In this paper, the uplink SE performance of a cell-free massive MIMO network has been evaluated in the presence of multiple distributed jammers. The SE has been compared with that of a UE in a single cell co-located massive MIMO. It was further compared with the SE of a UE in a cell-free system having smart jammers, in which each jammer individually contaminates one legitimate UE's channel estimate, as these jammers are supplied with all UEs' pilot signals. Furthermore, the SINR expressions for the above three scenarios have been derived in closed-forms by invoking the MRC detector and MMSE estimator. The simulation results demonstrated that cell-free massive MIMO outperforms co-located massive MIMO under the attacks of jammers. In addition, by comparing with the smart jammers scenario, the cell-free system with 5 passive jammers could achieve a better sum SE with probability 0.3. In order to enhance the SE, two designs for both pilot and data power coefficients were developed, with the aim to maximise the minimum SINR and to provide proportional fairness, respectively. The proportional fairness method demonstrated

a strong ability to increase the SE per UE and the sum SE compared with the full power case. On the other hand, the max-min fairness failed to provide good SE performance, as when a UE is highly affected by the jamming interference, a low SINR is obtained which reduces the uplink SE and the sum SE. Moreover, by changing the passive jammers' power, it has been shown that over 0 dBm is required to obtain a significant impact on the sum SE. However, this was not the case for the smart jammers which their harmful impacts started earlier than 0 dBm. Finally, at $\bar{\rho}_j = 45$ dBm, the sum SE with 5 passive jammers had the same SE of the smart jammers case.

APPENDIX

A. Derivation of (12)

This appendix includes the derivation of the SINR formula in (12). The expectation terms in (9a)-(9e) can be computed as:

1) Calculating DS_t: By depending on the properties of the MMSE estimation, $\hat{h}_{mt}$ and ε_{mt} are independent, thus, DS_t can be reformulated and computed as

$$\begin{aligned}\mathrm{DS}_t &= \sqrt{\rho_{u,t}}\,\mathbb{E}\left[\sum_{m=1}^{M}\hat{h}_{mt}^{*}(\hat{h}_{mt}+\varepsilon_{mt})\right]\\ &= \sqrt{\rho_{u,t}}\sum_{m=1}^{M}\mathbb{E}[\hat{h}_{mt}^{*}\hat{h}_{mt}] = \sqrt{\rho_{u,t}}\sum_{m=1}^{M}\theta_{mt}. \end{aligned} \tag{A1}$$

2) Calculating $\mathbb{E}[|\mathrm{IS}_1|^2]$: By applying the properties of variance of random variable, and by utilising the result of (A1), it can be demonstrated that

$$\begin{aligned}\mathbb{E}[|\mathrm{IS}_1|^2] &= \rho_{u,t}\mathbb{E}\left[\left|\sum_{m=1}^{M}\hat{h}_{mt}^{*}h_{mt} - \mathbb{E}\left[\sum_{m=1}^{M}\hat{h}_{mt}^{*}h_{mt}\right]\right|^2\right]\\ &= \rho_{u,t}\sum_{m=1}^{M}\left(\mathbb{E}\left[\left|\hat{h}_{mt}^{*}h_{mt}\right|^2\right] - \left|\mathbb{E}\left[\hat{h}_{mt}^{*}h_{mt}\right]\right|^2\right)\\ &= \rho_{u,t}\sum_{m=1}^{M}\left(\theta_{mt}\left(\beta_{mt}-\theta_{mt}\right) + 2\theta_{mt}^2 - \theta_{mt}^2\right)\\ &= \rho_{u,t}\sum_{m=1}^{M}\theta_{mt}\beta_{mt}. \end{aligned} \tag{A2}$$

3) Calculating $\mathbb{E}[|\mathrm{IS}_2|^2]$: As $\hat{h}_{mt}$ and h_{mk} are independent when $t \neq k$, and through following steps similar to those of (A2), $\mathbb{E}[|\mathrm{IS}_2|^2]$ can be computed as

$$\begin{aligned}\mathbb{E}[|\mathrm{IS}_2|^2] &= \rho_{u,k}\sum_{m=1}^{M}\mathbb{E}\left[\left|\hat{h}_{mt}^{*}h_{mk}\right|^2\right]\\ &= \rho_{u,k}\sum_{m=1}^{M}\mathbb{E}\left[\left|\hat{h}_{mt}^{*}\right|^2\right]\mathbb{E}\left[\hat{h}_{mk}^2+\varepsilon_{mk}^2\right]\\ &= \rho_{u,k}\sum_{m=1}^{M}\theta_{mt}(\theta_{mk}+\beta_{mk}-\theta_{mk}) = \rho_{u,k}\sum_{m=1}^{M}\theta_{mt}\beta_{mk}. \end{aligned} \tag{A3}$$

4) Calculating $\mathbb{E}[|\mathrm{JS}|^2]$: Similar steps to those used to derive (A2) can be employed her to prove that

$$\begin{aligned}\mathbb{E}[|\mathrm{JS}|^2] &= \bar{\rho}_j\sum_{m=1}^{M}\mathbb{E}\left[\left|\hat{h}_{mt}^{*}g_{mj}\right|^2\right]\\ &= \bar{\rho}_j\sum_{m=1}^{M}\mathbb{E}\left[\left|\hat{h}_{mt}^{*}\right|^2\right]\mathbb{E}\left[\left|g_{mj}\right|^2\right] = \bar{\rho}_j\sum_{m=1}^{M}\theta_{mt}\bar{\beta}_{mj}. \end{aligned} \tag{A4}$$

5) Calculating $\mathbb{E}[|\mathrm{NS}_t|^2]$: It can be shown

$$\mathbb{E}[|\mathrm{NS}_t|^2] = \sum_{m=1}^{M}\mathbb{E}\left[\left|\hat{h}_{mt}^{*}\right|^2\right]\sigma_t^2 = \sum_{m=1}^{M}\theta_{mt}\sigma_t^2. \tag{A5}$$

By combining (A2), (A3), and by substituting the results along all of (A1), (A4) and (A5) into (10), the SINR formula in (12) is obtained.

7. ACKNOWLEDGEMENT

The authors would like to thank the funding support by the EU Horizon 2020 Research and Innovation Programme, grant agreement no: 814956 (5G-DRIVE). The first author also gratefully acknowledges the wonderful friend Mrs Svenja Powell for the technical support that she kindly provided during the lockdown due to the COVID-19 pandemic.

REFERENCES

[1] H. Q. Ngo, A. Ashikhmin, H. Yang, E. G. Larsson, and T. L. Marzetta, "Cell-free massive MIMO: Uniformly great service for everyone," in *2015 IEEE 16th International Workshop on Signal Processing Advances in Wireless Communications (SPAWC)*, June 2015, pp. 201–205.

[2] ——, "Cell-free massive MIMO versus small cells," *IEEE Transactions on Wireless Communications*, vol. 16, no. 3, pp. 1834–1850, March 2017.

[3] H. Zhu, "Performance comparison between distributed antenna and microcellular systems," *IEEE Journal on Selected Areas in Communications*, vol. 29, no. 6, pp. 1151–1163, Jun. 2011.

[4] J. Wang, H. Zhu, and N. J. Gomes, "Distributed antenna systems for mobile communications in high speed trains," *IEEE Journal on Selected Areas in Communications*, vol. 30, no. 4, pp. 675–683, May. 2012.

[5] Z. Chen and E. Björnson, "Channel hardening and favorable propagation in cell-free massive MIMO with stochastic geometry," *IEEE Transactions on Communications*, pp. 1–1, 2018.

[6] H. Q. Ngo, L. Tran, T. Q. Duong, M. Matthaiou, and E. G. Larsson, "On the total energy efficiency of cell-free massive mimo," *IEEE Transactions on Green Communications and Networking*, vol. 2, no. 1, pp. 25–39, March 2018.

[7] R. Sabbagh, C. Pan, and J. Wang, "Pilot allocation and sum-rate analysis in cell-free massive MIMO systems," in *2018 IEEE International Conference on Communications (ICC)*, May 2018, pp. 1–6.

[8] D. Wang, M. Wang, P. Zhu, J. Li, J. Wang, and X. You, "Performance of network-assisted full-duplex for cell-free massive MIMO," *IEEE Transactions on Communications*, vol. 68, no. 3, pp. 1464–1478, 2020.

[9] D. Kapetanovic, G. Zheng, and F. Rusek, "Physical layer security for massive MIMO: An overview on passive eavesdropping and active attacks," *IEEE Communications Magazine*, vol. 53, no. 6, pp. 21–27, 2015.

[10] T. M. Hoang, H. Q. Ngo, T. Q. Duong, H. D. Tuan, and A. Marshall, "Cell-free massive MIMO networks: Optimal power control against active eavesdropping," *IEEE Transactions on Communications*, vol. 66, no. 10, pp. 4724–4737, 2018.

[11] X. Z. et al., "Secrecy analysis and active pilot spoofing attack detection for multigroup multicasting cell-free massive MIMO systems," *IEEE Access*, vol. 7, pp. 57 332–57 340, 2019.

[12] S. Timilsina, D. Kudathanthirige, and G. Amarasuriya, "Physical layer security in cell- free massive MIMO," in *2018 IEEE Global Communications Conference (GLOBECOM)*, 2018, pp. 1–7.

[13] J. Vinogradova, E. Björnson, and E. G. Larsson, "Detection and mitigation of jamming attacks in massive MIMO systems using random matrix theory," in *2016 IEEE 17th International Workshop on Signal Processing Advances in Wireless Communications (SPAWC)*, 2016, pp. 1–5.

[14] Z. Gülgün, E. Björnson, and E. G. Larsson, "Is massive MIMO robust against distributed jammers?" *IEEE Transactions on Communications*, vol. 69, no. 1, pp. 457–469, 2021.

[15] H. Zhu and J. Wang, "Chunk-based resource allocation in OFDMA systems - part I: chunk allocation," *IEEE Transactions on Communications*, vol. 57, no. 9, pp. 2734–2744, 2009.

[16] H. Zhu, "Radio resource allocation for OFDMA systems in high speed environments," *IEEE Journal on Selected Areas in Communications*, vol. 30, no. 4, pp. 748–759, 2012.

[17] S. M. Kay, *Fundamentals of Statistical Signal Processing: Estimation Theory*. USA: Prentice-Hall, Inc., 1993.

[18] T. L. Marzetta, E. G. Larsson, H. Yang, and H. Q. Ngo, *Fundamentals of Massive MIMO*. Cambridge University Press, 2016.

[19] T. T. Do, E. Björnson, E. G. Larsson, and S. M. Razavizadeh, "Jamming-resistant receivers for the massive MIMO uplink," *IEEE Transactions on Information Forensics and Security*, vol. 13, no. 1, pp. 210–223, 2018.

[20] S. Boyd and L. Vandenberghe, *Convex Optimization*. Cambridge University Press, 2004.

[21] M. Grant and S. Boyd, "CVX: Matlab software for disciplined convex programming, version 2.1," http://cvxr.com/cvx, Mar. 2014.

[22] "Evolved Universal Terrestrial Radio Access (E-UTRA); Further advancements for E-UTRA physical layer aspects (Release 9)," *3GPP Tech. Rep. 36.814*, March 2010.